

Weighing the Axion with Muon Haloscopy

N. Bray-Ali ^{a,1}

^a*Science Synergy,
Los Angeles, CA 90045, USA*

E-mail: nbrayali@gmail.com

ABSTRACT: Recent measurements of muon spin precession confirm a long-standing tension with the Standard Model of particle physics. We argue that axions from the local dark matter halo of the galaxy are responsible for the tension. The argument yields a percent level prediction for the mass of the axion provided that dark matter is made of axions. An analysis of charge asymmetry in kaon decays suggests that at least in the local halo dark matter is made of axions and that axions from the local halo are responsible for the observed violation by these reactions of the combined charge conjugation and spatial inversion symmetry operation. Tabletop experiments to directly detect dark matter in the form of axions with the proposed mass are proposed.

¹Corresponding author.

Contents

1	Introduction	1
2	Nature of Dark Matter	1
3	Kaon Haloscopy	2
4	Muon Haloscopy	2
5	Proton Haloscopy	4
6	Infrared Haloscopy	5
7	Conclusion	5

1 Introduction

The spin of the muon precesses in a magnetic field B at frequency $\omega_a = a_\mu(e/m_\mu)B$, where, $a_\mu \approx \alpha/(2\pi) \approx 1.16 \times 10^{-3}$ is the electromagnetic leading order contribution to spin precession, and $e/m_\mu = 2\pi \times 135$ MHz/T is the charge to mass ratio of the muon [1-4]. Compared with the electron, the muon is $(m_\mu/m_e)^2 \approx 43,000$ times more sensitive to the hadronic leading order contribution $a_\mu^{\text{HLO}} \approx 700 \times 10^{-10}$ to spin precession [5, 6]. In this Article, we show that axions in the local dark matter halo of the galaxy shift a_μ and a_μ^{HLO} from their standard model values. Further, we argue that the size of these axion-induced shifts explains the tension between measurements of the muon spin precession frequency [2, 3] and calculations of the frequency based on measurements of the hadronic leading order contribution [5] provided that dark matter in the local halo is made of axions as suggested by analysis of charge asymmetry between the kaon decay $K_L^0 \rightarrow \pi^+ e^- \bar{\nu}_e$ and its charge-parity conjugate $K_L^0 \rightarrow \pi^- e^+ \nu_e$ [7–11]. Finally, we give a physical picture for the nature of dark matter that leads to a prediction for the mass of the axion with percent level precision and we sketch table-top experiments for testing this prediction.

2 Nature of Dark Matter

We start by expressing the axion A_M in terms of quarks and leptons M_H^P with helicity $H = L, R$ and charge-parity check $P = +, -$ [13]:

$$A_M = M_L^- \bar{M}_R^- - M_R^- \bar{M}_L^- - M_L^+ \bar{M}_R^+ + M_R^+ \bar{M}_L^+ \quad (2.1)$$

Here, M runs over the twelve known “flavors” of quarks and leptons while the charge-parity check P is $+$ for quarks and leptons that do not feel the weak nuclear force and $-$ for those

that do. In the standard model, we find M_L^- and M_R^+ , but neither M_L^+ nor M_R^- , where, L is for left-handed and R is for right-handed helicity [14].

Next, we suppose that axions A_M of each kind and photons γ_H of each helicity formed in equal numbers in the early universe prior to baryogenesis. This fixes the ratio $n_A/n_\gamma = |M|/|H| = 6$ of axions to photons and gives the axion mass m_A ($\hbar = c = 1$) [15]:

$$m_A = 2.70 kT_\gamma \left(\frac{n_A}{n_\gamma} \right)^{-1} \frac{\Omega_A h^2}{\Omega_\gamma h^2} = (0.508 \pm 0.004) \text{ eV}, \quad (2.2)$$

where, $T_\gamma = (2.7255 \pm 0.0006) \text{ K}$ is the present photon temperature [16], $\Omega_\gamma h^2 = 2.473 \times 10^{-5}$ is the photon energy density parameter and $\Omega_A h^2 = 0.11882 \pm 0.00086$ is that of the axions assuming dark matter is made of axions [17].

3 Kaon Haloscopy

The energy density of axions in the local dark matter halo of the galaxy ρ_A can be estimated using the charge asymmetry of kaon decays [18]:

$$A_L(e) = -2\sqrt{2}\xi_{A\pi}p_K\tilde{\phi}_A(q_A) = 4\pi C_{A\pi} \frac{f_\pi\sqrt{\rho_A\hbar c}}{m_A f_A} L_K, \quad (3.1)$$

where, the axion amplitude $\tilde{\phi}_A(q_A)$ at momentum q_A changes sign under the combination of charge conjugation and space inversion probed by $A_L(e)$ to create the observed charge asymmetry [13]. The mixing angle $\xi_{A\pi} = -C_{A\pi}f_\pi/f_A$ between the axion A and the neutral pion π^0 can be expressed in terms of the pion decay constant $f_\pi = (92.32 \pm 0.09) \text{ MeV}$ [19], the axion decay constant f_A [20], and the light quark masses using $C_{A\pi} = (m_d - m_u)/(2m_u + 2m_d) = (0.173 \pm 0.08)$ [21]. Here, the kaon beam has momentum p_K and decays in-flight within a detector of length L_K .

Meanwhile, the axion mass m_A and the decay constant f_A only enter the kaon charge asymmetry through the product $m_A f_A = \sqrt{\chi_{\text{QCD}}} = (5.69 \pm 0.05) \times 10^{-3} \text{ GeV}^2$ which is fixed by the topological susceptibility χ_{QCD} of the quark chromodynamic vacuum [22]. Using the kaon parameters $L_K = 500 \text{ cm}$ and $A_L(e) = (3.32 \pm 0.08) \times 10^{-3}$ from the current best charge asymmetry measurement [12], the local axion energy density $\rho_A = (0.28 \pm 0.03) \text{ GeV/cm}^3$ that we find from Eq. (3.1) agrees with the best available estimate $\rho_{\text{DM}} = (0.30 \pm 0.03) \text{ GeV/cm}^3$ of the energy density of the local dark matter halo [23]. This agreement suggests that axions saturate the local dark matter halo and that dark matter from the local halo is the source of the charge asymmetry observed in kaon decays [24].

4 Muon Haloscopy

Figure 1 shows how axions in the local dark matter halo shift muon spin precession [2–4]. Acting as a background field $\tilde{\phi}_A(q_A)$ with on-shell four-momentum $q_A^2 = m_A^2 \ll m_\mu^2$, the axion A couples to the virtual photon dressing the vertex of the positive muon μ^+ and the

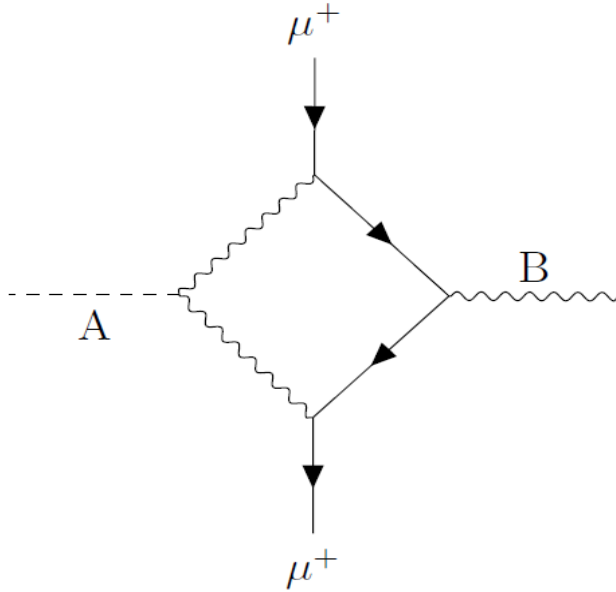


Figure 1. Halo axion A collides with virtual photon or vector meson dressing vertex of positive muon μ^+ and magnetic field B .

magnetic field B . The shift of the spin precession frequency Δa_μ goes as the strength of the coupling $g_{A\gamma\gamma}$ between the axion and a pair of photons [25]:

$$\frac{\Delta a_\mu}{a_\mu} = m_A^2 g_{A\gamma\gamma} \tilde{\phi}_A(q_A) = \pm m_A g_{A\gamma\gamma} \sqrt{\rho_A N_\mu V_\mu T_\mu} \quad (4.1)$$

where, the axion field strength $|\tilde{\phi}_A(q_A)|^2 \approx \phi_A^2 N_\mu V_\mu T_\mu$ is fixed by the axion energy density $\rho_A = \phi_A^2 m_A^2$, the volume V_μ of the muon beam, the lifetime T_μ of the muon in the axion rest-frame, and the average number of muons N_μ during spin precession. The sign of the shift Δa_μ in Eq. (4.1) switches along with the axion field $\tilde{\phi}_A(q_A)$ under spatial inversion P , under time-reversal T , and under the combinations CP and CT with charge conjugation C [26]. The size of the shift scales up with square root of the effective four-volume $\sqrt{N_\mu V_\mu T_\mu}$ of the muon beam.

The shift in the muon spin precession frequency Δa_μ due to axions in the local dark matter halo of the galaxy has roughly the right size to resolve the tension $a_\mu(\text{Exp}) - a_\mu(\text{SM}) = (251 \pm 59) \times 10^{-11}$ between experiments (Exp) [2, 3] and standard model calculations (SM) [5, 6]. The axion-photon coupling strength is $g_{A\gamma\gamma} = (0.68 \pm 0.02) \times 10^{-10} \text{ GeV}^{-1}$ for the axion mass $m_A = (0.508 \pm 0.004) \text{ eV}$ [27]. Combining these inputs, we find that the shift $\Delta a_\mu = (163 \pm 10) \times 10^{-11}$ of the muon spin precession frequency due to axions in the local dark matter halo roughly resolves the tension between experiment and the standard model [28].

Figure 1 also shows how axions from the local dark matter halo of the galaxy shift measurements of the leading order hadronic contribution a_μ^{HLO} to muon spin precession [4, 5]. The axions collide with the ρ^0 vector meson that dominates the hadronic production

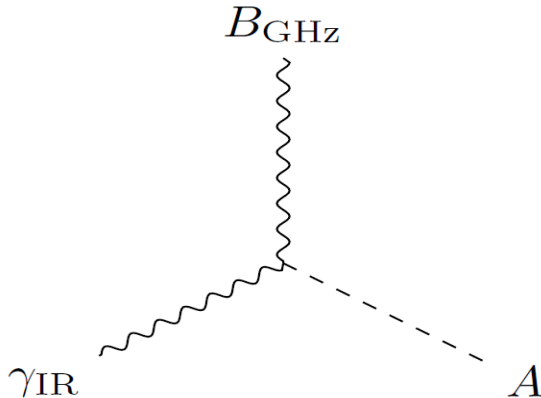


Figure 2. Halo axion A converts infrared photon γ_{IR} into microwave magnetic field B_{GHz}

from electron-positron annihilation whose cross-section enters the standard model calculation of a_μ^{HLO} . The collisions convert the short-lived ρ^0 meson, which produces mainly charged pion $\pi^+\pi^-$ pairs, into the longer lived and slightly heavier ω meson, which prefers to produce a neutral pion π^0 in addition to the charged pion pair. The conversions reduce the $\pi^+\pi^-$ hadronic production cross-section at the ρ^0 resonance and shift the calculated value of the leading order hadronic contribution by an amount set by the coupling $g_{A\rho\omega}$ of the axion to the ρ^0 and ω vector mesons [29]:

$$\begin{aligned} \frac{\Delta a_\mu^{\text{HLO}}}{a_\mu^{\text{HLO}}} &= m_A p_\rho g_{A\rho\omega} \tilde{\phi}_A(q_A) \\ &= \frac{\alpha}{3} \frac{\Delta a_\mu}{a_\mu} \frac{p_\rho}{m_A} \sqrt{\frac{m_\rho m_\omega}{\Gamma_\rho^{ee} \Gamma_\omega^{ee}} \frac{1}{N_\mu} \frac{V_e T_e}{V_\mu T_\mu}}, \end{aligned} \quad (4.2)$$

where, the mass of the vector meson $V = \rho, \omega$ is m_V , the partial width Γ_V^{ee} gives the rate that V produces an electron-positron pair, V_e is the luminous volume created by the colliding electron and positron bunches, T_e is the time it takes the bunches to cross during the collision, and p_ρ is the momentum of the ρ^0 vector meson in the axion rest frame. The shift $\Delta a_\mu^{\text{HLO}}$ in the hadronic contribution combines with the shift Δa_μ in the spin precession frequency to give a gap between experiment and the standard model $\Delta a_\mu + \Delta a_\mu^{\text{HLO}} = (311 \pm 18) \times 10^{-11}$ that is quite close to the observed tension [30].

5 Proton Haloscopy

Inverting the process shown in Figure 1 about a horizontal axis and replacing the muon with a proton, we find the way that axions from the local dark matter halo of the galaxy shift the spin precession of protons in liquid water [31]:

$$\Delta g_p' = \frac{\alpha}{\pi \epsilon} m_A^2 g_{A\gamma\gamma} \tilde{\phi}(q_A) = 2 \frac{\Delta a_\mu}{\epsilon} \sqrt{\frac{N_p V_p T_p}{N_\mu V_\mu T_\mu}}, \quad (5.1)$$

where, $\epsilon = 78.4$ [46] is the static dielectric constant of water and $g'_p \approx 2.79$ gives the proton spin precession frequency $\omega'_p = g'_p(e/m_p)B \approx 2\pi \times 42.8 \text{ MHz/T} \times B$ in liquid water for magnetic field B [32]. Here, N_p is the effective number of protons, V_p is the volume of the liquid water containing the protons, and $T_p = 1/\Delta\omega'_p$ is the effective coherence time of the proton spin precession due to the broadening $\Delta\omega'_p$ of the resonance by variations in the field strength over the sample volume. Straightforward estimates of the proton parameters give the slope of the axion shift of the proton spin precession frequency in water [33]:

$$\frac{1}{g'_p} \frac{dg'_p}{dT} = -(10.0 \pm 0.6) \text{ ppb/K} \left(\frac{V_p}{0.31 \text{ cm}^3} \right) \left(\frac{\Delta\omega'_p}{2.6 \times 10^{-7} \omega'_p} \right)^{-1/2}, \quad (5.2)$$

where, $T \approx 300 \text{ K}$ is the temperature of the liquid water. Measuring the slope dg'_p/dT would directly confirm in a tabletop experiment the proposed mechanism for the shift of spin precession by axions from the local dark matter halo with the predicted mass.

6 Infrared Haloscopy

Figure 2 shows how the axion converts infrared photons into microwave magnetic fields. From Eq. (2) we find that the wavelength $\lambda_A = 2\pi/m_A = (2441 \pm 19) \text{ nm}$ corresponding to the mass of the axion falls in the mid-infrared. Detuning the infrared light from λ_A by the ground-state hyperfine transition frequency of an alkali atom, such as cesium-133, we can create microwave magnetic field with strength [34]:

$$B_{\text{GHz}} = m_A^2 g_{A\gamma\gamma} E_{\text{IR}} \tilde{\phi}_A(q_A) = \frac{\Delta a_\mu}{a_\mu} E_{\text{IR}} \sqrt{\frac{N}{N_\mu} \frac{V_{\text{IR}}}{V_\mu} \frac{T_{\text{IR}}}{T_\mu}}. \quad (6.1)$$

Here, E_{IR} is the infrared electric field strength, N is the number of gas atoms, V_{IR} is the volume of the infrared beam within the gas cell, and T_{IR} is the coherence time of the light. By scanning the infrared wavelength and looking for resonant absorption of the microwave magnetic field by the atoms, it is possible to measure λ_A and hence determine the mass of the axion directly in a table-top experiment to better than a percent.

Figure 3 shows how the axion allows infrared light to excite electromagnons in ferroelectric antiferromagnets such as BiFeO_3 . At room temperature the strongest electromagnon resonance in BiFeO_3 lies in the terahertz regime at frequency $\omega_\theta = 2\pi \times 0.54 \text{ THz}$ [35]. Looking in the infrared, we expect to see the electromagnon resonance as an absorption line in transmission through a thin sample, for example, provided the light is detuned by ω_θ from the axion frequency $\omega_A = m_A = 2\pi \times (122.9 \pm 1.0) \text{ THz}$ [36]. Measuring the infrared frequency that resonantly excites the electromagnon provides a table-top determination of the mass of the axion to better than a percent.

7 Conclusion

We conclude that the tensions between measurements of muon spin precession and standard model calculations are due to axions from the local dark matter halo of the galaxy. The

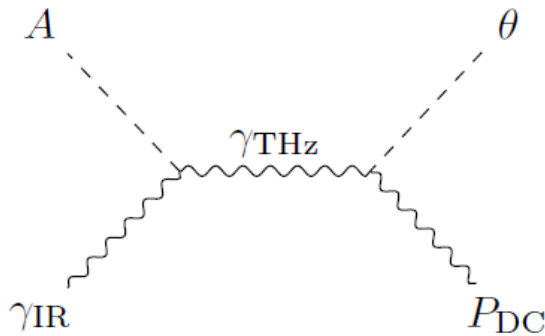


Figure 3. Halo axion A converts infrared photon γ_{IR} into terahertz photon γ_{THz} resonant with electromagnon θ in ferroelectric antiferromagnet with polarization P_{DC} .

resolution of the muon tension rests on a novel physical picture for the nature of dark matter. The picture leads to percent level predictions for the mass of the axion and for its coupling to electromagnetic fields provided that dark matter is made of axions.

Using kaon decays, we showed that dark matter in the local halo of the galaxy is made of axions. The observed charge asymmetry in kaon decays agrees with the asymmetry created by axions provided the axions have energy density that matches that of the local dark matter halo. The agreement suggests that the kaon decay asymmetry is due to axions in the local dark matter halo and that the local halo is made of axions.

The shift in the muon spin precession frequency due to axions from the local dark matter halo depends not just on the local axion energy density but also on the axion mass and electromagnetic coupling strength. For the mass of the axion predicted by our novel physical picture of the nature of dark matter, the predicted shift in the muon spin precession explains about half the observed tension between precession measurements and calculations based on measurements of the hadronic contribution. The other half of the tension follows from the analogous shift by axions of the measurements of the hadronic contribution: Axions from the local dark matter halo convert the neutral vector meson that dominates photon-hadron interactions into its slightly heavier and less dominant isoscalar cousin. Combining the two axion shifts, we resolve the muon tension provided that axions have the predicted mass.

Finally, we have proposed table-top experiments to confirm that axions shift spin precession and to directly measure the mass of the axion. Measurements of the volume dependence of the drop in the proton spin precession resonance frequency with increasing temperature in liquid water would confirm the proposed mechanism for axions to shift spin precession. Similarly, observing resonant interference between infrared light and axions from the local dark matter halo at the predicted wavelength would confirm that dark matter is made of axions not just locally but also cosmologically.

Acknowledgements

This research was supported in part by the National Science Foundation under Grant No. NSF PHY-1748958, by the Department of Energy under grant No. DE-FG02-00ER41132, and by the Mainz Institute of Theoretical Physics within the Cluster of Excellence PRISMA+ (Project ID 39083149).

Open Access. This article is distributed under the terms of the Creative Commons Attribution License ([CC-BY 4.0](https://creativecommons.org/licenses/by/4.0/)), which permits any use, distribution and reproduction in any medium, provided the original author(s) and source are credited. SCOAP³ supports the goals of the International Year of Basic Sciences for Sustainable Development.

References

- [1] J. Schwinger, *On Quantum-Electrodynamics and the Magnetic Moment of the Electron*, Phys. Rev. **73** (1948) 416.
- [2] B. Abi, T. Albahri, S. Al-Kilani, D. Allspach, L. P. Alonzi et al. (Muon $g - 2$ Collaboration), *Measurement of the Positive Muon Anomalous Magnetic Moment to 0.46 ppm*, Phys. Rev. Lett. **126** (2021) 141801.
- [3] G.W. Bennett, B. Bousquet, H. N. Brown, G. Bunce, R. M. Carey et al. (Muon $g - 2$ Collaboration), *Final report of the muon E821 anomalous magnetic moment measurement at BNL*, Phys. Rev. D **73** (2006) 072003.
- [4] F. Jegerlehner, *The Anomalous Magnetic Moment of the Muon*, 2nd ed., Springer-Verlag, Berlin (2017).
- [5] T. Aoyama, N. Asmussen, M. Benayoun, J. Bijnens, T. Blum et al., *The anomalous magnetic moment of the muon in the standard model*, Phys. Rep. **887** (2020) 1.
- [6] Sz. Borsanyi, Z. Fodor, J. N. Guenther, C. Hoelbling, S. D. Katz et al., *Leading hadronic contribution to the muon magnetic moment from lattice QCD*, Nature **593** (2021) 51.
- [7] P. A. Zyla et al. (Particle Data Group), *Review of Particle Physics*, Prog. Theor. Exp. Phys., **2020** (2020) 083C01.
- [8] S. Bennett et al., Phys. Rev. Lett. **19** (1967) 993.
- [9] J. Marx et al., Phys. Lett. B **32** (1970) 219.
- [10] V. L. Fitch et al. Phys. Rev. Lett. **31** (1973) 1524.
- [11] C. Geweniger et al., Phys. Lett. B **48** (1974) 483.
- [12] A. Alavi-Harati et al. (FNAL KTeV Collab.), Phys. Rev. Lett. **88** (2002) 181601.
- [13] The axions A_M are constructed to transform under C , P , and T as follows:

$$CA_M = A_M, PA_M = -A_M, TA_M = -A_M.$$

To check that they do so, recall that quarks and leptons M_H^P transforms as follows:

$$CM_H^P = \overline{M_H^P}, PM_H^P = M_H^P, TM_H^P = \overline{M_H^P}.$$

- [14] For anti-matter, the meaning of the parity check is reversed compared to matter: $P = +$ indicates anti-quarks and anti-leptons which *do* feel the weak force, while $P = -$ means the anti-matter *does not* feel it. Nevertheless, the standard model correlation between helicity $H = L, R$ and parity check $P = +, -$ applies in the same way to anti-matter as it does to matter: \overline{M}_L^- and \overline{M}_R^+ occur in the standard model while neither \overline{M}_L^+ nor \overline{M}_R^- do. See, for example, the discussion in Ref. [38] on pgs. 704–705.
- [15] There are $|M| = 12$ flavors of matter in the standard model of particle physics. They fall into three “generations” each containing a pair of quarks and a pair of leptons. See the discussion in Ref. [38] on pgs. 703–705, 707, and 721 for a detailed description of the matter content of the Standard Model in the language of quantum field theory. The ratio of the energy density parameters $\Omega_A h^2 / (\Omega_\gamma h^2) = u_A / u_\gamma$ gives the ratio of the energy per volume $u_A = m_A n_A$ stored in dark matter to the energy per volume $u_\gamma = 2.70 \times n_\gamma k T_\gamma$ stored in light energy. For a derivation, see P. J. E. Peebles, *Principles of Physical Cosmology*, Princeton University Press, Princeton, NJ (1993), pgs. 137–138, 158–160. The Boltzmann constant is [39]:

$$k = 1.380\,649 \times 10^{-23} \text{ J/K (exact)} = 0.861\,733 \times 10^{-4} \text{ eV/K.}$$

- [16] D. J. Fixsen, The Temperature of the Cosmic Microwave Background, *Astrophys. J.* **707** (2009) 916.
- [17] N. Aghanim, Y. Akrami, M. Ashdown, J. Aumont, C. Baccigalupi et al. (Planck Collaboration), *Planck 2018 Results VI. Cosmological Parameters*, *A&A* **641** (2018) A6. We use parameters from the baseline model fit to the most complete combination of available data. The results are given in *Planck 2018 Results: Cosmological Parameter Tables*, pg. 49 (May 14, 2019).
- [18] The rate $\Gamma(\pi^- e^+ \nu_e)$ of the decay of the long-lived neutral kaon K_L^0 to a negative pion π^- , a positron e^+ , and an electron neutrino ν_e is larger than the rate $\Gamma(\pi^+ e^- \bar{\nu}_e)$ for the charge conjugate reaction due to the charge asymmetry [7]:

$$A_L(e) = (\Gamma(\pi^- e^+ \nu_e) - \Gamma(\pi^+ e^- \bar{\nu}_e)) / (\Gamma(\pi^- e^+ \nu_e) + \Gamma(\pi^+ e^- \bar{\nu}_e)) = (3.34 \pm 0.07) \times 10^{-3}.$$

The axion field strength $|\tilde{\phi}_A(q_A)|^2 \approx \phi_A^2 V_K T_K$ is fixed by the axion energy density $\rho_A = \phi_A^2 m_A^2$ where ϕ_A is the axion amplitude as a function of position [20]. The kaon volume $V_K = \pi L_K (h/p_K)^2$ and the kaon time $T_K = L_K/c$ give the size of the region of space-time within the decay volume where the axion and kaon interact coherently. The following exact values for the defining constants of the international system (SI) appear in the expression for $A_L(e)$ and/or in its numerical evaluation [39]:

$$\begin{aligned} c &= 299\,792\,458 \text{ m/s,} \\ h &= \hbar \times 2\pi = 6.626\,070\,15 \times 10^{-34} \text{ J s,} \\ e &= 1.602\,176\,634 \times 10^{-19} \text{ C.} \end{aligned}$$

- [19] J. L. Rosner, S. L. Stone and R. Van de Water, *71. Leptonic decays of charged pseudoscalar mesons*, pg. 803 in Ref. [7] gives the result $|V_{ud}| f_\pi \times \sqrt{2} = 127.13 \pm 0.13 \text{ MeV}$ where $|V_{ud}| = 0.973\,70 \pm 0.000\,14$ is the light quark mixing amplitude [40]. Combining we find $f_\pi = (92.32 \pm 0.09) \text{ MeV}$ for the pion decay constant.
- [20] R. D. Peccei, in *CP Violation*, ed. C. Jarlskog, World Scientific, Singapore (1989), pgs. 525–532.
- [21] $C_{A\pi}$ follows from the way the axion shifts $U_\theta \phi_A = \phi_A + 2\theta f_A$ under the axial twist $U_\theta M_H^P = e^{-iP\theta} M_H^P$ in the phase of matter that feels the weak nuclear force M_H^- relative to

the phase of matter M_H^+ that does not feel this force. See Ref. [20] for $C_{A\pi}$ in terms of the light quark masses and the way the axion shifts under the axial twist. See Ref. [41] for the light quark mass ratio $m_u/m_d = 0.485 \pm 0.019$.

- [22] M. Gorghetto and M. Villadoro, *Topological susceptibility and QCD axion mass: QED and NNLO corrections*, J. High Energ. Phys. **2019** (2019) 33.
- [23] A.-C. Eilers, D. W. Hogg, H.-W. Rix, and M. K. Ness, *The Circular Velocity Curve of the Milky Way from 5 to 25 kpc*, Astrophys. J. **871** (2019) 120.
- [24] Using the value for $\rho_A = (0.28 \pm 0.03) \text{ GeV/cm}^3$ determined by the best available $A_L(e)$ measurement in Ref. [12], one can use Eq. (3.1) to predict the charge asymmetry observed in other experiments given the length L_K of their decay volume. For example, the first such measurement $A_L(e) = (2.24 \pm 0.36) \times 10^{-3}$ [8] had length $L_K = 375 \text{ cm}$ which yields $A_L(e) = (2.46 \pm 0.17) \times 10^{-3}$ using Eq. (3.1) in pleasing agreement with the observed charge asymmetry despite the well-known tension of this first measurement with the current world average. The difference in the length L_K resolves the tension. The rough similarity in the length $L_K \approx 500 \text{ cm}$ of the measurements that enter the current world average for which published scale drawings of the decay volume are available [9, 11, 12] explains the consistency of their results for $A_L(e)$ given the relation with L_K expressed in Eq. (3.1).
- [25] The axion ϕ_A couples to photons via the term in the action

$$\mathcal{S}_{A\gamma} = \int d^3x dt g_{A\gamma\gamma} \phi_A \mathbf{E} \cdot \mathbf{B}$$

where, \mathbf{E} is the electric field and \mathbf{B} is the magnetic field. We follow here the conventions of Ref. [20] in which the “free” terms in the axion action take the form

$$\mathcal{S}_A = \int d^3x dt [(1/2)(\partial_t \phi_A)^2 - (1/2)(\nabla \phi_A)^2 - (1/2)m_A^2 \phi_A^2].$$

- [26] Under C , PT and CPT , the shift Δa_μ , like the axion amplitude, does not change sign.
- [27] The axion-photon coupling is given by the following expression [20, 25]:

$$g_{A\gamma\gamma} = C_{A\gamma} \frac{\alpha}{2\pi} \frac{1}{f_A} = (0.68 \pm 0.02) \times 10^{-10} \text{ GeV}^{-1}. \quad (7.1)$$

Here, the fine-structure constant enters [39]:

$$\alpha = (7.297\ 352\ 5693 \pm 0.000\ 000\ 00011) \times 10^{-3}. \quad (7.2)$$

The mass of the axion m_A and the product $m_A f_A = \sqrt{\chi_{\text{QCD}}}$ which is fixed by the topological susceptibility χ_{QCD} of the quark chromodynamic vacuum combine to give the axion decay constant [22]:

$$f_A = \frac{m_A f_A}{m_A} = \frac{(5.69 \pm 0.05) \times 10^{-3} \text{ GeV}^2}{(0.508 \pm 0.004) \text{ eV}} = (1.120 \pm 0.010) \times 10^7 \text{ GeV}. \quad (7.3)$$

Finally, the light quark mass ratio $m_u/m_d = 0.485 \pm 0.019$ [41] gives the dimensionless constant [20, 25]:

$$C_{A\gamma} = \frac{8}{3} - \frac{2}{3} \frac{4m_d + m_u}{m_d + m_u} = 0.653 \pm 0.017. \quad (7.4)$$

- [28] For the muon beam at Fermilab E989 (FNAL) [2], the volume is

$$V = 2\pi^2 R \sigma_x \sigma_y = 3.12 \times 10^4 \text{ cm}^3,$$

where, $R = 711$ cm is the radius of the central orbit of muons in the ring, $\sigma_x = 1.78$ cm is the radial width of the beam, and $\sigma_y = 1.25$ cm is the vertical width [2, 42, 43]. The average number of muons is

$$N = \frac{4}{9} N_0 e^{-t_{\text{fill}}/(\gamma\tau_\mu)} \approx \frac{4}{9} \times 4340 = 1930,$$

where, $N_0 \approx 6920$ is the number of muons in the ring at the start of the fill, and $t_{\text{fill}} \approx 30$ μsec is the time it takes to fill the ring [2, 42]. The muon life-time in the haloscope rest frame is $T = \gamma_\mu \tau_\mu = 64.4$ μsec , where, $\gamma_\mu \approx p_\mu/(m_\mu c) = 29.3$ is the muon time dilation factor, $p_\mu = 3.10$ GeV/c is the muon momentum, $m_\mu = 0.106$ GeV/c² is the muon rest mass, and $\tau_\mu = 2.20$ μsec is the muon life-time at rest [2]. For the measurements at Brookhaven E821 (BNL) [3], we estimate $N = 1290$, $\sigma_x = 2.10$ cm, $\sigma_y = 1.53$ cm (J. Mott, private communication). To find the shift of muon spin precession from halo axions, we first computed $|\Delta a_\mu(\text{FNAL})| = (165 \pm 10) \times 10^{-11}$ and $|\Delta a_\mu(\text{BNL})| = (161 \pm 10) \times 10^{-11}$ for each experiment using Eq. (3). Next we took the average of the two experiments to obtain Δa_μ , since the shifts essentially agree.

[29] We follow the analysis reviewed in Ref. [20] and set the ratio of axion couplings

$g_{A\rho\omega}/g_{A\gamma\gamma} = g_{\pi\rho\omega}/g_{\pi\gamma\gamma}$ to match that of the neutral pion. Vector meson dominance [44] gives the pion ratio in terms of the ρ and ω vector meson partial widths for electron-positron pair production, as shown in Eq. (4). The electron-positron quantities entering Eq. (4) may be expressed in terms of the collider parameters: $V_e = 8\pi\sigma_x\sigma_y\sigma_z$ where $\sigma_x, \sigma_y, \sigma_z$ are the horizontal, vertical, and longitudinal sizes of the bunch at the interaction point, $T_e = 2\sigma_z/c$, and the ρ^0 vector meson has momentum $p_\rho = (E^2 - m_\rho^2)/(2E)$ in the lab frame for annihilation of electrons and positrons with equal beam energies $E_+ = E_- = E/2$ that collide after emitting a photon with energy $E - m_\rho$. For example, the DAΦNE collider had $E_+ = E_- = m_\phi/2 = 510$ MeV and used initial state radiation to reach the ρ^0 vector meson resonance for $\pi^+\pi^-$ creation from e^+e^- annihilation [45]. For energy scan experiments, the collision energy $E \approx m_\rho$ lands on the ρ^0 vector meson resonance, and, as a result, the ρ^0 vector meson has lab-frame momentum $p_\rho = \sqrt{2} \times \Delta E$ set by the spread ΔE in the beam energy.

[30] The meson parameters are as follows [7]:

$$\begin{aligned} m_\rho &= 775 \text{ MeV}, \\ m_\omega &= 783 \text{ MeV}, \\ \Gamma_\rho^{ee} &= \Gamma_\rho \times \text{B.R.}(\rho \rightarrow e^+e^-) = (147 \text{ MeV})(4.72 \times 10^{-5}) = 6.94 \text{ keV}, \\ \Gamma_\omega^{ee} &= \Gamma_\omega \times \text{B.R.}(\omega \rightarrow e^+e^-) = (8.68 \text{ MeV})(7.38 \times 10^{-5}) = 0.641 \text{ keV}. \end{aligned}$$

Using the meson parameters, we can find the vector meson coupling strengths [44]:

$$\begin{aligned} g_\rho^2/(4\pi) &= \alpha^2 m_\rho / (3\Gamma_\rho^{ee}) = 1.98, \\ g_\omega^2/(4\pi) &= \alpha^2 m_\omega / (3\Gamma_\omega^{ee}) = 21.7. \end{aligned}$$

These coupling strengths then give the ratio of the axion-meson coupling to the axion-photon coupling [20, 44]:

$$\frac{g_{A\rho\omega}}{g_{A\gamma\gamma}} = \frac{1}{\alpha} \sqrt{\frac{g_\rho^2}{4\pi} \frac{g_\omega^2}{4\pi}} = 8.98 \times 10^2.$$

The axion coupling ratio allows us to evaluate the drop in the hadronic contribution (See Eq.

4):

$$\begin{aligned}\Delta a_\mu^{\text{HLO}} &= \Delta a_\mu \left(\frac{a_\mu^{\text{HLO}}}{a_\mu} \right) \left(\frac{p_\rho}{m_A} \right) \left(\frac{g_{A\rho\omega}}{g_{A\gamma\gamma}} \right) \sqrt{\frac{1}{N_\mu} \frac{V_e}{V_\mu} \frac{T_e}{T_\mu}} \\ &= 0.170 \times \Delta a_\mu (\text{FNAL}) \left(\frac{p_\rho}{100 \text{ MeV}} \right) \left(\frac{V_e}{10^{-2} \text{ cm}^3} \right)^{1/2} \left(\frac{T_e}{100 \text{ psec}} \right)^{1/2},\end{aligned}$$

where, we have approximated the standard model value for the muon spin precession by the leading order electromagnetic contribution $a_\mu \approx \alpha/(2\pi) \approx 1.16 \times 10^3$ [1, 4, 5]. Similarly, we approximate the standard model value for the hadronic contribution to muon spin precession $a_\mu^{\text{HLO}} = 700 \times 10^{-10}$ [5, 6]. The muon beam parameters N_μ , V_μ , and T_μ are those of the FNAL E989 spin precession experiment [28]. Hadron production by the DAΦNE collider detected by KLOE at the ρ^0 vector meson $\pi^+\pi^-$ resonance lies close to the world average for this channel which dominates the a_μ^{HLO} calculation within the standard model [5]. We therefore estimate the shift $\Delta a_\mu^{\text{HLO}}$ using the electron-positron beam parameters inside KLOE at DAΦNE [45]:

$$\sigma_x = 0.2 \text{ cm}, \sigma_y = 2 \times 10^{-3} \text{ cm}, \sigma_z = 3 \text{ cm}, E_+ = E_- = 510 \text{ MeV}.$$

Combining the electron-positron beam parameters using the expressions in [29], one finds $V_e = 3.0 \times 10^{-2} \text{ cm}^3$, $T_e = 200 \text{ psec}$, and $p_\rho = 219 \text{ MeV}$. Finally, we get the shift of the hadronic contribution at KLOE:

$$\Delta a_\mu^{\text{HLO}}(\text{KLOE}) = 0.170 \times (165 \pm 10) \times 10^{-11} \times 2.19 \times \sqrt{(3.0)(2.0)} = (148 \pm 9) \times 10^{-11},$$

where, we have used the shift $\Delta a_\mu(\text{FNAL})$ predicted using FNAL E989 beam parameters [28].

- [31] Figure 1 shows the leading order quantum electrodynamic radiative correction to the electromagnetic vertex of the proton in water [46]:

$$\Delta g'_{p,\text{EM}} = \frac{\alpha}{\pi\epsilon} \approx \frac{1}{137 \times \pi \times 78.4} \approx 2.96 \times 10^{-5}. \quad (7.5)$$

This correction dominates the axion shift since the axion needs to couple to a virtual photon. By contrast, hadronic contributions dominate the full radiative correction to the electromagnetic vertex of the proton in liquid water [32]:

$$g'_p - 2 \approx 2.79 - 2 = 0.79. \quad (7.6)$$

Despite dominating the full electromagnetic vertex correction, these hadronic contributions do not contain the necessary virtual photon. Thus, they make a sub-dominant contribution to the axion shift of the proton spin precession frequency in water.

- [32] W. D. Phillips, W. E. Cooke and D. Kleppner, *Magnetic Moment of the Proton in H₂O in Bohr Magnetons*, Phys. Rev. Lett. **35** (1975) 1619; *ibid.* **36** (1976) 689 and 1473.
 [33] The bulb of liquid water in Ref. [32] was a sphere of diameter 1.3 cm with volume

$$V_p = (4\pi/3)(1.3/2)^3 \text{ cm}^3 = 1.15 \text{ cm}^3. \quad (7.7)$$

The proton resonance line-width $\Delta\omega'_p = 2\pi \times 1.5 \text{ Hz}$ due to variation in the field strength over the sample volume gave effective spin coherence time

$$T_p \approx 1/\Delta\omega'_p = 0.11 \text{ sec}. \quad (7.8)$$

The temperature of the bulb $T = (34.7 \pm 0.1)^\circ\text{C} = 308 \text{ K}$ gave proton spin polarization

$$P_p = \frac{\hbar\omega'_p}{kT} = \frac{4.14 \times 10^{-9} \text{ eV/MHz} \times 15 \text{ MHz}}{0.862 \times 10^{-4} \text{ eV/K} \times 308 \text{ K}} = 2.34 \times 10^{-6}, \quad (7.9)$$

where, the precession frequency was $\omega'_p = 2\pi \times 42.8 \text{ MHz/T} \times 0.35 \text{ T} = 15 \text{ MHz}$ in magnetic field $B = 0.35 \text{ T}$ [32]. Using the proton volume V_p and proton polarization P_p , we find the effective proton number

$$\begin{aligned} N_p &= n_p V_p P_p \\ &= (6.69 \times 10^{22} \text{ cm}^{-3}) \times (1.15 \text{ cm}^3) \times (2.34 \times 10^{-6}) \\ &= 1.80 \times 10^{17}, \end{aligned} \quad (7.10)$$

where, we have used the proton number density in liquid water

$$n_p = (1.00 \text{ g/cm}^3)(6.02 \times 10^{23} \text{ H}_2\text{O}/18.0 \text{ g})(2 \text{ p/H}_2\text{O}) = 6.69 \times 10^{22} \text{ cm}^{-3}. \quad (7.11)$$

Using Eq. (5.1), we find the shift of the proton spin precession frequency in water:

$$\begin{aligned} \Delta g'_p &= 2 \times \frac{(165 \pm 10) \times 10^{-11}}{78.4} \left(\frac{1.80 \times 10^{10}}{1.93 \times 10^3} \right)^{1/2} \left(\frac{1.15 \text{ cm}^3}{3.12 \times 10^4 \text{ cm}^3} \right)^{1/2} \left(\frac{0.11 \text{ sec}}{64.4 \times 10^{-6} \text{ sec}} \right)^{1/2} \\ &= (1.02 \pm 0.06) \times 10^{-4} \left(\frac{V_p}{1.15 \text{ cm}^3} \right) \left(\frac{T_p}{308 \text{ K}} \right)^{-1/2} \left(\frac{\Delta\omega'_p}{10^{-7} \omega'_p} \right)^{-1/2}, \end{aligned} \quad (7.12)$$

where, $\epsilon = 78.4$ [46] is the static dielectric constant in water and we have taken the muon beam parameters N_μ, V_μ, T_μ and the predicted shift Δa_μ from the Fermilab E989 muon spin precession measurement [28]. Taking the temperature derivative, we find the slope

$$\frac{1}{g'_p} \frac{dg'_p}{dT} = -\frac{1}{2} \frac{\Delta g'_p}{g'_p T} = -(60 \pm 4) \times 10^3 \text{ ppb/K} \left(\frac{V}{1.15 \text{ cm}^3} \right) \left(\frac{T}{308 \text{ K}} \right)^{-3/2} \left(\frac{\Delta\omega'_p}{10^{-7} \omega'_p} \right)^{-1/2}, \quad (7.13)$$

where, $g'_p \approx 2.79$ gives the slope in parts per billion (ppb) of g'_p [32].

- [34] The radio-frequency magnetic field points along the infrared electric field.
- [35] D. Talbayev, S. A. Trugman, Seongsu Lee, Hee Taek Yi, S.-W. Cheong, and A. J. Taylor, *Long-wavelength magnetic and magnetoelectric excitations in the ferroelectric antiferromagnet BiFeO₃*, Phys. Rev. B **83** (2011) 094403.
- [36] The electromagnon θ resonates when the terahertz electric field E_{THz} is perpendicular to the spin cycloid plane in BiFeO₃. This plane is defined by the spontaneous polarization P_{DC} and the cycloid wavevector: See Eq. (10), Fig. 2, and accompanying discussion on pg. 3 of Ref. [37]. The axion converts the magnetic field B_{IR} in the incident infrared light into a parallel terahertz frequency electric field E_{THz} . The infrared light gets absorbed when E_{THz} resonates with the electromagnon θ . This happens when B_{IR} is perpendicular to the spin cycloid plane.
- [37] R. de Sousa and J. E. Moore, *Optical coupling to spin waves in the cycloidal multiferroic BiFeO₃*, Phys. Rev. B **77** (2008) 012406.
- [38] M. E. Peskin and D. V. Schroeder, *An Introduction to Quantum Field Theory*, Perseus, Cambridge, MA (1995).
- [39] D. B. Newell et al. (CODATA), *Metrologia* **55** (2018) L13.
- [40] A. Ceccucci, Z. Ligeti, and Y. Sakai, *12. CKM Quark-Mixing Matrix*, pg. 262 in Ref. [7].

- [41] Z. Fodor, C. Hoelbig, S. Krieg et al., *Up and Down Quark Masses and Corrections to Dashen's Theorem from Lattice QCD and Quenched QED*, Phys. Rev. Lett. **117** (2016) 082001.
- [42] T. Albahri, A. Anastasi, K. Badgley, S. Baessler, I. Bailey et al. (Muon $g - 2$ Collaboration), *Beam dynamics corrections to the Run-1 measurement of the muon anomalous magnetic moment at Fermilab*, Phys. Rev. Accel. Beams **24** (2021) 044002.
- [43] T. Albahri, A. Anastasi, A. Anisenkov, K. Badgley, S. Baessler et al. (Muon $g - 2$ Collaboration), *Measurement of the anomalous precession frequency of the muon in the Fermilab Muon $g - 2$ Experiment*, Phys. Rev. D **103** (2021) 072002 .
- [44] R. P. Feynman, *Photon-Hadron Interactions*, Addison-Wesley, Redwood City, CA (1972), pgs. 82–85 introduce the vector meson coupling strengths

$$g_V = \alpha \sqrt{4\pi m_V / (3\Gamma_V^{e e})}$$

for $V = \rho, \omega$ and pgs. 96–97 express the pion amplitude ratio

$$g_{\pi\rho\omega} / g_{\pi\gamma\gamma} = g_\rho g_\omega / (4\pi e^2)$$

in terms of these couplings and the electric charge e . Note that $e^2 = \alpha \approx 1/137$ in Feynman's conventions.

- [45] F. Ambrosino et al. (KLOE Collaboration), *Measurement of the DAΦNE luminosity with the KLOE detector using large angle Bhabha scattering*, Eur. Phys. J. C **47** (2006) 589.
- [46] D. P. Fernandez, Y. Mulev, A. R. Goodwin and J. M. H. Levelt Sengers, *Database for the Static Dielectric Constant of Water and Steam*, J. Phys. Chem. Ref. Data **24** (1995) 33, Table 2 gives the static dielectric constant $\epsilon = 78.43 \pm 0.10$ for liquid water at room temperature $T = 298.14$ K and atmospheric pressure $P_a = 10^5$ Pa by averaging over published measurements of the dielectric response at frequencies ranging from 100 Hz to 40 GHz. The quoted uncertainty is the population standard deviation of these measurements about their average value.